

Vacancy effects in the x-ray photoelectron spectra of  $\text{TiN}_x$ 

Louis Porte

*Laboratoire de Physico-Chimie Minérale, Laboratoire (No. 116) associé au Centre National de la Recherche Scientifique, Université de Lyon I, 43 boulevard du 11 novembre 1918, F-69622 Villeurbanne, France*

Laurent Roux and Jean Hanus

*Groupe de Physique des Etats Condensés, Equipe (No. 373) de Recherche associé au Centre National de la Recherche Scientifique, Faculté des Sciences de Luminy, Université d'Aix-Marseille II, F-13288 Marseille, France*

(Received 27 December 1982)

The electronic structures of titanium nitrides  $\text{TiN}_x$  have been investigated by x-ray photoelectron spectroscopy over the entire composition range of the rocksalt structure ( $0.5 \leq x \leq 1$ ). The valence-region spectrum of stoichiometric TiN is consistent with results of band-structure calculations. The filling of a defect state at about 2-eV binding energy with decreasing  $x$  is explicitly demonstrated. Experimental results are compared with different models for calculation of the electronic structure of anion-deficient rocksalt transition-metal compounds. Variation of the core-level binding energies indicates a decrease of the ionicity in  $\text{TiN}_x$  with decreasing  $x$ . The Ti 2*p* satellite structure found for nearly stoichiometric samples is discussed in terms of screening of the core hole by the conduction electrons.

## I. INTRODUCTION

Transition-metal carbides and nitrides have long been of special interest due to their unusual combination of physical and chemical properties.<sup>1,2</sup> They display high melting point, ultrahardness, and good corrosion resistance—properties which are typical of covalent crystals—as well as thermal and electrical conductivities comparable to those of pure transition metals. This remarkable behavior has prompted a number of band-structure calculations<sup>3–7</sup> which now provide good understanding of these materials. The calculations show that the nonmetal 2*s* states (at about 11 eV below the Fermi energy for the carbides, and 15 eV for the nitrides) are well separated from the valence-band structure at 5–6 eV below the Fermi energy that is built up from nonmetal 2*p* states which are strongly hybridized with metal *d* states. The density of states (DOS) falls to a minimum corresponding to the completion of the hybridized *p-d* states, then rises again due to states having mainly metal *d* character. The filling of these states and the position of the Fermi level is determined basically by the total number of valence electrons, i.e., in TiC (eight valence electrons) the Fermi level will be at a minimum of DOS, while in TiN (nine valence electrons) some *d*

states are filled and the Fermi level occurs in a higher DOS region. Many experimental studies have demonstrated the essential features of this model to be correct for both the carbides<sup>8</sup> and the nitrides. Studies of the electronic structures of the transition-metal nitrides involve spectroscopies such as x-ray photoelectron spectroscopy (XPS),<sup>9</sup> ultraviolet photoemission spectroscopy,<sup>9–11</sup> angle-resolved photoelectron spectroscopy,<sup>12,13</sup> electron-energy loss spectroscopy,<sup>11</sup> x-ray emission,<sup>14–17</sup> and absorption,<sup>16–18</sup> and optical spectroscopies.<sup>19,20</sup> Studies on carbonitrides have also been reported.<sup>21,22</sup>

The ability of the transition-metal carbides, nitrides, and oxides to exist over a wide range of stoichiometries is another remarkable feature of these compounds. Vacancies can be introduced into the nonmetal fcc sublattice, but for the oxides where vacancies are also present in the metal fcc sublattice. The physical properties of the compound are modified by the introduction of vacancies, and the understanding of the electronic structure in a nonstoichiometric compound represents a particularly interesting challenge. The possible influence of the vacancies on the electronic structure depends markedly on the theoretical model used. According to some theoretical models,<sup>23–25</sup> one of the most important effects of the vacancies is the creation of

new filled states in the nonstoichiometric compound. Other theoretical models,<sup>26,27</sup> however, do not predict these new states but suggest that electrons introduced by anion deficiency occupy the conduction band. Despite the very large field of investigations offered by the nonstoichiometric transition-metal compounds, experimental results on the electronic structure are yet limited,<sup>9,11,20,28-30</sup> and very few<sup>9,28</sup> have focused on the controversy relating to the creation of new states. As the departure from the stoichiometry can be very large in the transition-metal compounds under consideration, it appeared to us that an investigation covering the entire composition range of a nonstoichiometric NaCl phase would be particularly profitable. Titanium nitride is then a good candidate since the rocksalt phase is obtained over a wide range of composition from  $\text{TiN}_{0.5}$  to  $\text{TiN}_{1.1}$ . XPS is well adapted to electronic structure studies since it is a very efficient probe of the DOS of a compound.

This paper reports the first XPS study of  $\text{TiN}_x$  to cover the entire composition range of the NaCl phase. Section II deals with experimental procedure, special attention being given to the contamination problem which can have drastic effects on the XPS results of these compounds. Section III presents the results; in particular, we focus attention on the experimental valence-band structures in relation to the different theoretical approaches to the vacancy problem. The effect of vacancies on the XPS core-level peaks is also discussed.

## II. EXPERIMENTAL

One major difficulty when studying substoichiometric vacancy compounds such as  $\text{TiN}_x$  is to obtain materials free of bulk or surface contaminants. The study of single crystals would probably represent an optimal approach. Unfortunately, monocrystals have been grown only for selected nearly stoichiometric compositions, and strongly nitrogen-deficient crystals cannot be obtained by established procedures. As an alternative, the sputtering technique is of interest since it allows the preparation of  $\text{TiN}_x$  films with nitrogen content varying over the entire composition range of the rocksalt phase. Moreover, film preparation in a clean vacuum limits the level of contamination. The  $\text{TiN}_x$  samples studied in the present work were polycrystalline thin films ( $\sim 2000$  Å thick) deposited by reactive sputtering from a Ti target in an Ar- $\text{N}_2$  atmosphere onto Mo substrates heated at  $300^\circ\text{C}$ .<sup>31</sup> X-ray diffractometry demonstrated the presence of a single NaCl phase, whose cubic lattice parameter increased with increasing nitrogen content.<sup>1</sup> The composition of selected films was obtained by nuclear-

reaction microanalysis. These values provided the reference points for  $x$  standardization of the compositions derived from XPS measurements, using the intensity ratios between the N 1s and Ti 2p core peaks. The XPS stoichiometries obtained in such a way are in good agreement with the nominal stoichiometries, the deviation on the nitrogen content  $x$  being less than  $\pm 0.03$  units over the whole range of  $\text{TiN}_x$  compositions. The stoichiometries reported in the text are based on XPS. They are truly representative of the surface region investigated in the XPS experiment (typically about 50 Å). Note also that their relative precision is only dependent on the statistical precision of the experimental data, enabling the composition parameter  $x$  in  $\text{TiN}_x$  to be determined to within  $\pm 0.02$ .

The XPS spectra were taken with a Vacuum Generators ESCA III spectrometer using the unmonochromatized  $\text{MgK}\alpha$  radiation ( $h\nu = 1253.6$  eV). The experimental resolution was 1.1 eV. The base pressures in the analyzer and the preparation chambers were  $10^{-10}$  Torr. Prior to the measurements, the surface of the sample was very slightly argon etched in order to remove the natural protective titanium-dioxide coating. Then the samples were annealed at about 1100 K by electronic bombardment to ensure the removal of possible implanted argon and the reconstruction of a crystalline surface with proper stoichiometry. During the annealing, the pressure was not allowed to rise beyond  $3 \times 10^{-9}$  Torr. Note that annealing the sample without removing the titanium-dioxide coating might induce some undesirable contamination of the  $\sim 2000$ -Å-thick  $\text{TiN}_x$  layer through the diffusion of oxygen atoms into it. After the annealing, the presence of weak O 1s and C 1s core peaks revealed the presence of small amounts of oxygen and carbon contaminants. This is not surprising, as the nuclear reaction microanalysis proved the layers to contain around 1–2 % of oxygen or carbon atoms. The C 1s signal due to carbon species adsorbed on the surface was easily distinguished from that due to carbon in lattice sites.<sup>30</sup> Comparison with the C 1s signal from a titanium-carbide sample demonstrated that the carbon level probed by XPS is similar to the bulk value found by nuclear microanalysis. The O 1s signals from oxygen adsorbed on the surface and oxygen bound into lattice sites have indistinguishable binding energies. However, previous experiments on the adsorption of oxygen on titanium<sup>32</sup> give us confidence that the O 1s signal comes mainly from adsorbed oxygen. In particular, the intensity of the O 1s signal was increased by tilting the sample to ensure acceptance of electrons at small angles of photoemission. Nuclear microanalysis and XPS

core-level analysis leads us to estimate that the oxygen amount in the bulk should not exceed 3%.

Figure 1 shows the XPS valence-band spectra from titanium oxynitride, titanium carbonitride, and titanium nitride samples. In the two former spectra, the signals originating from O 2s- and C 2s-like states are easily identified at binding energies around 23 and 12 eV, respectively. (The binding energies refer to the Fermi level.) Even though small amounts of carbon and oxygen contaminants may, in principle, induce some distortion in the  $\text{TiN}_x$  XPS valence band, we may take our data to be representative of a pure  $\text{TiN}_x$  phase provided that there are no detectable O 2s and C 2s signals.

Höchst *et al.*<sup>9</sup> suggested that an annealing procedure was inappropriate to the cleaning of substoichiometric titanium nitrides as it would produce only the stoichiometric composition near the surface. Our results provide clear contrary evidence of the efficiency of the annealing procedure in cleaning nonstoichiometric materials. Of the range of  $\text{TiN}_x$  compositions we studied, the only sample signifi-

cantly modified by prolonged annealing was titanium-deficient  $\text{TiN}_{1.03}$ . This sample lost nitrogen to yield a film with composition near that of  $\text{TiN}_{0.8}$ . With lower nitrogen concentrations, only small variations in stoichiometry could also be detected after prolonged annealing. But as it is possible to determine the stoichiometry by XPS core-level analysis, this is more an advantage than a trouble since it allows one to follow the evolution of the XPS as a function of small change in the  $\text{TiN}_x$  stoichiometry.

### III. RESULTS AND DISCUSSION

#### A. Evolution of the valence-band structure in $\text{TiN}_x$

Figure 2 shows the XPS valence band of nearly stoichiometric titanium nitride  $\text{TiN}_{0.97}$ . The background arising from secondary electrons has been subtracted in order to facilitate comparison with the DOS calculated for stoichiometric TiN by Neckel *et al.*<sup>5</sup> The positions of the three main peaks at 16.6, 6, and 0.6 eV are in good enough agreement with the theoretical calculation, which allows us to identify respective maxima in the DOS due to a nearly pure N 2s band, a valence N 2p band originat-

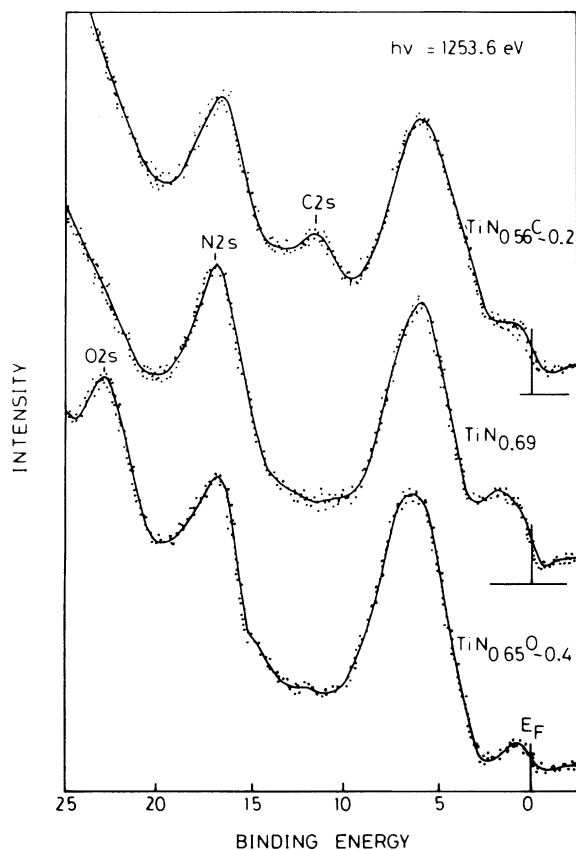


FIG. 1. Valence-band photoemission spectra from titanium oxynitride (low), titanium nitride (middle), and titanium carbonitride (high) samples.

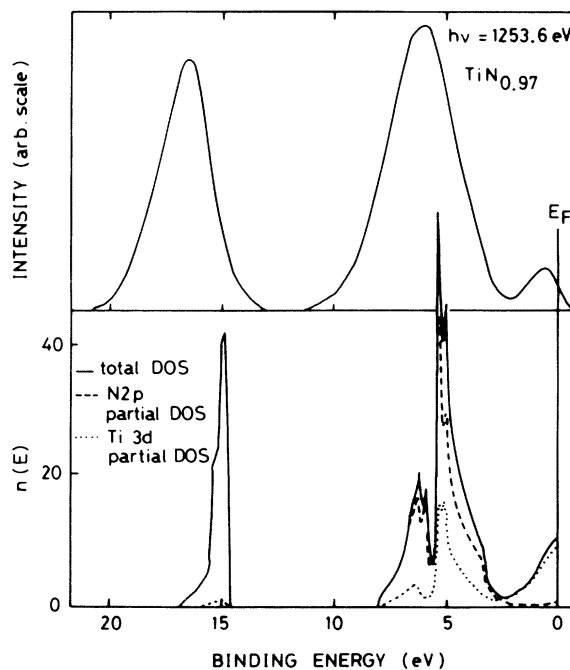


FIG. 2. Valence-band photoemission spectra of  $\text{TiN}_{0.97}$  after subtraction of the secondary electrons' background. Comparison with the total and partial DOS from Ref. 5. The partial N 2s DOS is nearly equivalent to the total DOS peak at 15-eV binding energy.

ing from mixed nitrogen  $p$  and metal  $d$  states, and a nearly pure metal  $d$  conduction band weakly mixed with nitrogen  $p$  states. Our spectrum is in good agreement with that previously reported for stoichiometric TiN by Höchst *et al.*<sup>9</sup> using monochromatic AlK $\alpha$  radiation. It also resembles spectra recorded by Johansson *et al.*<sup>10</sup> using synchrotron radiation in the energy range of 70–190 eV, and classical HeI and HeII resonance radiations. The only discrepancy between experimental spectra and calculation is a slightly smaller value of the N2s binding energy for the latter.

Surprisingly, the relative intensities of the three main bands are difficult to understand on the basis of the Gelius model<sup>33</sup> of partial DOS weighted by the differential atomic photoionization cross sections. The high intensity of the N2s band in the x-ray photoelectron spectra conforms with the high photoionization cross section for N2s levels relative to N2p and Ti3d levels reported in Scofield's calculations.<sup>34</sup> The surface intensity ratio between the N2s- and Ti3d-like bands also conforms quite reasonably with the theoretical N2s to Ti3d cross-section ratio. But the intensity of the 6-eV structure is too high to be reconcilable with the theoretical N2p–Ti3d cross-section values. A possible cause of intensity enhancement of the 6-eV structure could be oxygen surface adsorption. However, the relative intensity of the structures in the spectra reported by Höchst *et al.*<sup>9</sup> does not differ substantially from ours, though these authors noted no trace of surface contamination. It is equally remarkable that the TiN valence band recorded with different uv lines<sup>9</sup> do not display the marked dependence of relative intensities upon energy of the incident radiation which is expected from cross-section calculations.<sup>35</sup> One would anticipate an increase in the 3d band intensity and a decrease in the 2p valence-band intensity as  $h\nu$  increases. Höchst *et al.*<sup>28</sup> have also reported that a very large enhancement of the C2p photoionization cross section above its atomic value must be postulated in order to account for the intensity of the hybridized  $p$ - $d$  band in the XPS from NbC. It is generally considered that band intensities in XPS are governed by partial DOS weighted by an atomic cross section: In the XPS regime the dominant contributions to valence-level photoionization matrix elements are expected to come from regions near the nucleus where the wave functions should be free-atom-like.<sup>33,35</sup> It seems, however, that the applicability of the model to compounds like TiN or NbC, where there is strong band hybridization, may be questionable.

Figure 3 shows the evolution of the XPS valence band with the composition parameter  $x$  in TiN $_x$

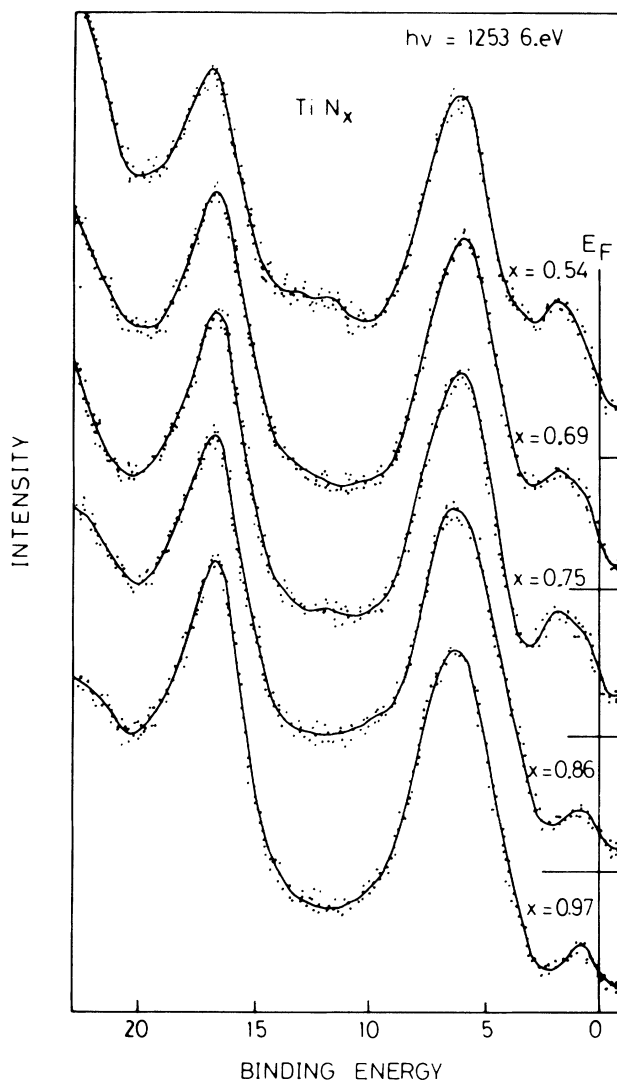


FIG. 3. Valence-band photoemission spectra of TiN $_x$ : evolution with the stoichiometry. All spectra have been normalized to the Ti3p core-level intensity.

( $0.54 < x < 0.97$ ). The main features are as follows. First, the decrease in the intensity of the N2s band with decreasing nitrogen content is in quite satisfactory agreement with TiN $_x$  stoichiometry. This behavior is not unexpected in view of the nearly pure N2s character of this band. Second, the total intensity of the  $d$ -like band, between 0 and 2.5 eV, increases as  $x$  decreases. This can be qualitatively understood on the basis of the simple picture: As  $x$  decreases, the number  $n$  of available  $p$  states ( $n = 6x$ ) decreases, less  $d$  electrons can be accommodated in the  $p$  band and a progressively larger number are transferred to higher unoccupied  $d$  states. It transpires, however, that this crude model is unable

to take account for the detailed structure of the  $d$  band (see below). Finally, the band structure around 6 eV appears only little affected by the change in  $\text{TiN}_x$  stoichiometry. This could be due to some compensating effect of the differential photoionization cross sections on the strongly hybridized  $p$ - $d$  states of the band.

We focus now on a more detailed discussion of the two lowest-lying bands. Typical spectra are shown in Fig. 4(a). The increase in intensity of the  $d$  band with decreasing nitrogen content originates mainly from the appearance of a new structure at around 2-eV binding energy, where there is a valley in the DOS for stoichiometric TiN. The concomitant increase of DOS at the Fermi level is rather small. The spectra also exhibit a slight narrowing of the  $N$   $2p$ -like band as  $x$  decreases. The new structure was first noted by Höchst *et al.*<sup>9</sup> in their study of a single-crystal  $\text{TiN}_{0.8}$ . After verification that this structure could not be attributed to metal segregation at the surface or to oxygen adsorption at the vacant sites, they concluded that it originated from occupied defect states. Our results confirm the earlier work (see, for example, the effect of oxygen in Fig. 1) and demonstrate additionally that changes in the "defect" structure correlate with the stoichiometry. In particular, the intensity of the new peak increases with the nitrogen vacancy concentration, strongly supporting its assignment to an occupied defect state. Höchst *et al.*<sup>28</sup> also noted the appearance of an additional structure at about 1.9 eV below the Fermi level in the XPS of  $\text{NbC}_{0.85}$  which was not present in the XPS of  $\text{NbC}_{0.96}$ .

The great difficulty in theoretical calculations of the electronic structure of nonstoichiometric materials is due in large part to the problem of taking proper account for the lattice vacancies. Various approaches have been developed, especially for rocksalt-structure transition-metal compounds. DOS calculations have been done by Klima for  $\text{TiC}_x$  (Ref. 26) and  $\text{TiN}_x$ ,<sup>36</sup> and by Klein *et al.*<sup>27</sup> for  $\text{NbC}_x$ ,  $\text{TaC}_x$ , and  $\text{HfC}_x$ . These authors used the coherent potential approximation (CPA) in a linear combination of atomic orbitals basis. Cluster calculations have been performed by Schwartz and Röscher<sup>37</sup> for niobium carbide, and by Ries and Winter<sup>25</sup> for niobium carbide and vanadium nitride using the multiple-scattering self-consistent-field (SCF)  $X\alpha$  approximation. Recently, energy-band structure and DOS have been obtained by Wimmer *et al.*<sup>24</sup> for the long-range-ordered vacancy compound  $\text{Nb}_{0.75}\text{O}_{0.75}$ . They carried out self-consistent calculations for the real  $\text{Nb}_{0.75}\text{O}_{0.75}$  structure as well as for stoichiometric NbO with a hypothetical NaCl structure using the augmented-plane-wave (APW)

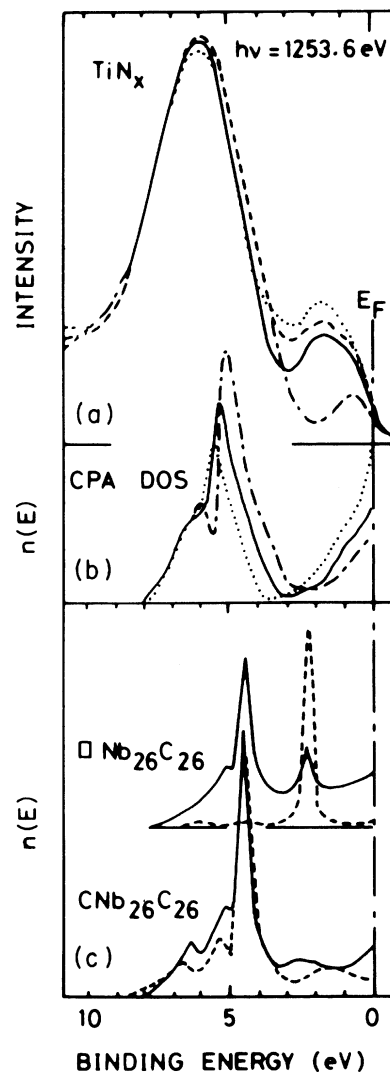


FIG. 4. Comparison of  $\text{TiN}_x$  valence-band photoemission spectra with CPA and cluster calculations. All spectra have been aligned on the Fermi energy. (a) Experimental spectra normalized to the Ti  $3p$  core-level intensity.  $x = 0.94$ , ---;  $x = 0.75$ , —;  $x = 0.69$ , - - -;  $x = 0.54$ , . . . . Note the increase of the new structure at  $\sim 2$  eV binding energy with decreasing  $x$ . (b)  $\text{TiN}_x$  density of states from CPA calculations (Ref. 36).  $x = 1$ , ---;  $x = 0.8$ , —;  $x = 0.6$ , . . . . (c) SCF  $X\alpha$  partial DOS in 53-atom NbC cluster from Ref. 25. Low is without vacancy. C site:  $n_p^{(000)}$ , ---; Nb site:  $N_d^{(100)}$ , —; high is with C(000) vacancy. C site:  $n_p^{\text{vac}}$ , - - -; Nb site:  $N_d^{(100)}$ , —.

method.

Klima's calculations<sup>36</sup> are of particular interest to us since they represent the only theoretical study of  $\text{TiN}_x$  over its entire composition range. The computed total DOS are shown in Fig. 4(b). All the curves have been aligned on the Fermi level in order

to make comparison with the experimental spectra. CPA calculations verify simple arguments based on a rigid-band picture. Removing a nitrogen atom decreases the number of N  $2p$  states, liberating three electrons per N atom which are transferred to empty  $d$  states above the Fermi level of the stoichiometric compound. Thus the Fermi level rises and the DOS at the Fermi level  $n(E_F)$  increases with decreasing nitrogen content. Though the experimental spectra exhibit this variation of  $n(E_F)$ , it is much less than predicted by CPA calculations. Magnetic susceptibility or specific-heat-capacity measurements allow a determination of the DOS at the Fermi level and would be relevant for comparison. We are not aware of such experiments for  $\text{TiN}_x$ , but paramagnetic susceptibilities have been reported for the analogous system  $\text{ZrN}_x$ .<sup>38</sup> Here there is qualitative agreement with CPA calculations and XPS results in that the paramagnetic susceptibility of  $\text{ZrN}_x$  increases with decreasing  $x$ .

CPA calculations predict a Fermi-level shift of 0.5 eV from  $\text{TiN}$  to  $\text{TiN}_{0.6}$ . This behavior is hardly noticeable from XPS where only a very small change in the position of the  $p$  bands relative to the Fermi level can be observed. The major visible discrepancy between the CPA DOS, and the XPS spectra relates to the failure of the calculations to predict the new defect structure between  $p$ - and  $d$ -like states for substoichiometric compounds. In the CPA calculations the vacancies are modeled by setting their energy  $\epsilon^v = \infty$ , which is equivalent to eliminating the terms in the Hamiltonian corresponding to allowed electron hopping to the vacant site. Huisman *et al.*<sup>23</sup> have proposed a quite different approach to the vacancy problem in their study of the mechanism for vacancy stabilization in  $\text{TiO}$  and  $\text{TiC}$ . They chose  $\epsilon^v$  to have a small finite value, thus permitting an electron to have a nonzero amplitude on a vacant site. In this model the presence of vacancies in the  $\text{TiO}$  lattice produces a new band of defect states to appear between the O  $2p$  band and the Ti  $3d$  band. These states are associated with the interactions occurring in the metallic cluster of titanium which forms around an anion vacancy. In this connection, real-space approaches such as cluster calculations are of great interest, as an alternative to band-structure calculations which are seriously complicated when the translation symmetry is destroyed by vacancy formation. However, we are aware only of published DOS calculations for NbC clusters.<sup>25,37</sup> NbC is relevant as a material for qualitative comparison with  $\text{TiN}$  as the two compounds are isoelectronic and APW calculations reveal that their DOS profiles are strikingly similar.<sup>5,39</sup> In particular, the same two groups of DOS peaks are

found for NbC (Ref. 39) as for  $\text{TiN}$ ,<sup>5</sup> with the metal  $d$ -like states near the Fermi level and the anion  $p$ -like states at around 5–6 eV binding energy. The main differences are more pronounced  $p$ - $d$  mixing in the carbide and a slight destabilization of the C  $2p$ -like band relative to the N  $2p$ -like band of  $\text{TiN}$ . In Fig. 4(c) the results of SCF  $X\alpha$  calculation for the NbC cluster are shown, with and without carbon vacancy.<sup>25</sup> When a carbon vacancy is introduced into the 53-atom cluster, a new level appears at around 2-eV binding energy. The corresponding wave function has a dominant contribution from an  $s$ -like wave in the vacant carbon sphere, but also has significant amplitude on the six Nb(100) atoms adjacent to the vacancy. This result provides strong evidence that the structure around 2 eV in the XPS of substoichiometric  $\text{TiN}_x$  is due to vacancy states.

The calculations of Wimmer *et al.*<sup>24</sup> on stoichiometric niobium monoxide  $\text{Nb}_{0.75}\text{O}_{0.75}$  provide additional insight into the vacancy problem. This compound crystallizes in a structure which is derived from that of NaCl but with 25% vacancies on each sublattice. As the vacancies have long-range order, it was possible to perform calculations using rigorous, well-established band-structure methods. As the primitive unit cell for  $\text{Nb}_{0.75}\text{O}_{0.75}$  contains three NbO units, nine O  $p$  bands were expected in the energy-band structure. Actually, one more supplementary band was found in the energy range spanned by the O  $p$  bands. This band, which mostly lies below the Fermi energy, is induced by the vacancies and is mainly occupied with electrons originating from Nb  $d$ -like wave functions. In the DOS of  $\text{Nb}_{0.75}\text{O}_{0.75}$ , this "vacancy band" gives a well-defined structure, mainly  $d$ -like in character, lying between the Fermi energy and the structure built up from the O  $p$  states. Comparison of the  $\text{Nb}_{0.75}\text{O}_{0.75}$  DOS and of the DOS obtained for the hypothetical fully stoichiometric NbO compound makes clear evidence of the appearance of this new structure in  $\text{Nb}_{0.75}\text{O}_{0.75}$ . The maximum intensity of the new structure occurs at around 1.5 eV below the Fermi energy. Despite the fact that vacancies in  $\text{TiN}_x$  are not ordered, this provides additional theoretical support to the argument that vacancies induce supplementary structure in the DOS profile. These new states are situated below the conduction band of the stoichiometric compound and must be filled before the narrow conduction band. Thus the intensity of the vacancy band in XPS [the feature 2 eV below  $E_F$  in Fig. 4(a)] increases with increasing anion vacancy concentration. Note also that  $n(E_F)$  increases much more slowly than expected from the CPA calculations, which fail to take proper account of the creation of new vacancy states.

### B. Ionicity, electronic localization, and stoichiometry

We turn now to analysis of core-level spectra which reveal interesting changes with varying stoichiometry. The binding-energy shift relative to the Fermi energy  $\Delta E_B$  of Ti  $2p$  core lines between metallic Ti and TiN has been found equal to 1.2 ( $\pm 0.1$ ) eV, in agreement with previous reports.<sup>9,40,41</sup> Neckel *et al.*<sup>5</sup> computed the charge transfer for TiN. It emerged from their APW calculations that there was transfer of around  $\frac{1}{3}$  electron per Ti atom from titanium to nitrogen spheres, in qualitative agreement with the measured core-level shifts. In nitrogen-deficient materials, the Ti  $2p$  core-level shifts  $\Delta E_B$  decrease from 1.2 eV in TiN to a minimum value of 0.7 eV in TiN<sub>0.5</sub>. Chemical shifts of the Ti  $L_{II,III}$  x-ray emission lines reported by Holliday<sup>14</sup> on the TiN<sub>x</sub> series show very similar variation. Höchst *et al.*<sup>9</sup> do not mention any change in the core-level binding energies between TiN and TiN<sub>0.8</sub>, but the XPS chemical shift between these two compositions is small and possibly within the range of the experimental uncertainty. Stoichiometry-dependent chemical shifts in XPS have also been reported for the metal core lines from several transition-metal carbides series.<sup>30,40,42</sup>

The interpretation of core-level shifts in terms of charge transfer is difficult because other effects such as changes in crystal potential, relaxation energy, and reference level may also introduce shifts in core-level binding energies. In the case of the series TiN<sub>x</sub>, an alternative is to consider the difference of binding energies between the Ti  $2p_{3/2}$  photopeak and the N  $1s$  photopeak. The plot of this difference as a function of the TiN<sub>x</sub> stoichiometry (Fig. 5) is actually more informative of the variation of the charge transfer since differences in relaxation energies for Ti and N core holes should be similar, and reference-level effects are no longer relevant. Calculations show that the crystal potential cannot induce a very significant change in the N  $1s$ –Ti  $2p_{3/2}$  binding-energy difference with varying TiN<sub>x</sub> composition (typically less than 0.1 eV). Figure 5 shows an increase in the N  $1s$ –Ti  $2p_{3/2}$  difference with  $x$ . This behavior truly reflects an increase in charge transfer from titanium to nitrogen as  $x$  is increased. A simple model for the bonding in transition-metal compounds<sup>6</sup> provides a means of analyzing the effect of removing nitrogen from the TiN lattice. In the NaCl-like structure the Ti  $3d$ - $eg$  orbitals are pointed towards the N  $2p$  orbitals enabling anion-cation  $\sigma$  overlap. The Ti  $3d$ - $t2g$  orbitals overlap to some extent with the N  $2p$  orbitals in a  $\pi$ -like fashion. The strong covalent mixing of cation and anion levels explains the refractory properties of

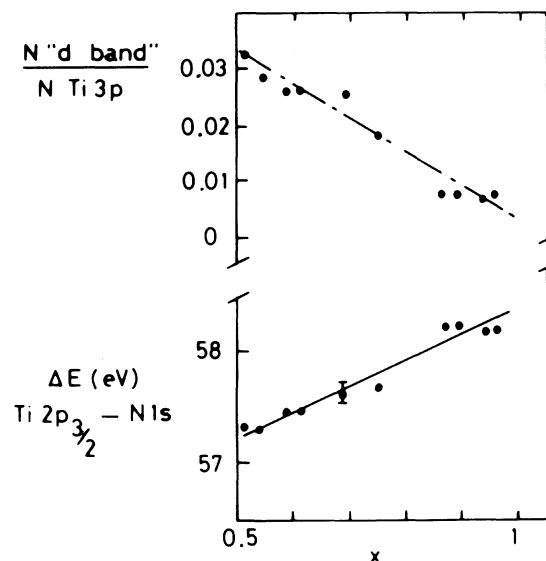


FIG. 5. Binding-energy difference between the Ti  $2p_{3/2}$  and the N  $1s$  core peaks vs the TiN<sub>x</sub> stoichiometry (low). Intensity ratio between the  $d$  band and the Ti  $3p$  core peak vs the TiN<sub>x</sub> stoichiometry (high). The intensity of the  $d$  band is estimated from XPS valence-band spectra by subtraction of the secondary electrons' background and stripping of the N  $2p$ -like band structure.

these materials. Partial ionic character also occurs in the bonding, as shown by the progressive decrease of refractory character from TiC, through TiN, to TiO.<sup>43</sup> Increasing the ionic character, with the electronegativity difference, leads to lowering of the cohesive energy of the crystal. Metal-metal  $\sigma$  bonding occurring through the overlap of the Ti  $3d$ - $t2g$  orbitals of neighbor titanium atoms mediates the metallic electrical conductivity of these materials. Removing a nitrogen atom allows the six titanium atoms surrounding the vacancy to regain some of the electron density they had originally transferred as a result of bonding, thus decreasing the net charge transfer in the material. In our qualitative band model it was seen that the electrons left behind after the departure of a nitrogen atom are accommodated in higher states either of the Ti  $3d$ - $t2g$  band near the Fermi level or in the vacancy states. In Fig. 5 we also show estimates of the number of  $d$  states obtained from the XPS valence-band spectra after subtraction of the background and stripping of the N  $2p$ -like band structure. The aim here is to show the correspondence between core-level and valence-band measurements: As  $x$  decreases, the ionicity decreases and the electronic population of

states belonging chiefly to the metal increases.

We turn finally to discuss the shape of the titanium core peaks. The Ti 2*p* signals recorded for different TiN<sub>x</sub> compositions are shown in Fig. 6. A striking feature is the appearance of a strong satellite structure at around 2.2 eV to the high binding-energy side of the Ti 2*p* doublet lines for compositions approaching the stoichiometric value. This additional structure is also found in the Ti 3*p* spectra, but as the Ti 3*p*<sub>1/2</sub>–Ti 3*p*<sub>3/2</sub> doublet is not resolved, it manifests itself in a broadening of the Ti 3*p* photopeaks. To our knowledge there exist only three publications referring to XPS core-level measurements on TiN.<sup>9,40,41</sup> Höchst *et al.*<sup>9</sup> did not mention satellite structure but the Ti 2*p* spectra were not shown. The Ti 2*p* spectrum reported by Simon *et al.*<sup>41</sup> is unfortunately obscured by the Ti 2*p* signal from a TiO<sub>2</sub> layer covering their inadequately cleaned TiN sam-

ple. The Ti 2*p* of the TiN spectrum shown by Ramqvist *et al.*<sup>40</sup> contains a satellite structure at around 2.5 eV from the main Ti 2*p*<sub>1/2-3/2</sub> lines, attributed to signals originating from an oxidized surface. However, the binding energies are smaller than those from TiO<sub>2</sub> (by about 1 eV, as far as we can estimate from their figure). Throughout extensive investigation of the oxidation of titanium,<sup>32,44</sup> and of titanium carbides, nitrides, or oxides,<sup>45</sup> we have never seen Ti 2*p* signals originating from an oxidized surface whose binding energy was not very close to that of TiO<sub>2</sub> itself. We presume, consequently, that the satellite structures in the spectrum of Ramqvist *et al.* have the same origin as those in Fig. 6.

Complex core-level structure has been encountered in the photoelectron spectra of a wide range of metallic materials, including tungsten bronzes,<sup>46,47</sup> metallic oxides,<sup>48</sup> alloys,<sup>49,50</sup> and simple metals.<sup>51</sup> The interpretation of these satellites is by no means uncontroversial, and radically different interpretations have been advocated. For example, W 4*f* satellites in the sodium-tungsten bronzes have been taken to indicate, on one hand, the presence of several valence states in the initial state of the material,<sup>47</sup> and on the other, to represent final-state effects in the photoemission process.<sup>46,52</sup> The occurrence of different valence states in the initial state does not seem consistent with the itinerant properties of the conduction electrons or with strong covalent bonding in materials such as the tungsten bronzes or the titanium nitrides. Satellite structures in XPS may have various possible causes<sup>53</sup> and qualitative interpretation may often be obtained by resorting to different theoretical approaches. However, good quantitative agreement with theory is more difficult to find, as shown by the exhaustive treatment from Chazalviel *et al.*<sup>46</sup> on the problem of the W 4*f* satellites in the Na<sub>x</sub>WO<sub>3</sub> series. To some extent the titanium-nitrides series present some similarity with the sodium-tungsten bronzes series, as the number of electrons entering the conduction band can be varied along with the stoichiometry.

Ionization of a core subshell produces a strong electrostatic perturbation which can pull down a localized state from the conduction band.<sup>54</sup> This localized state can become occupied or remain empty in the XPS transition, thus corresponding to the observed main line and satellite line, respectively. This model is attractive because it allows one to link the relative intensity between satellite and the main line to the occupancy of the conduction band: The probability of filling the localized state depends on the occupancy of the band. Fuggle *et al.*<sup>49</sup> restated this problem in terms of core-hole screening. If an elec-

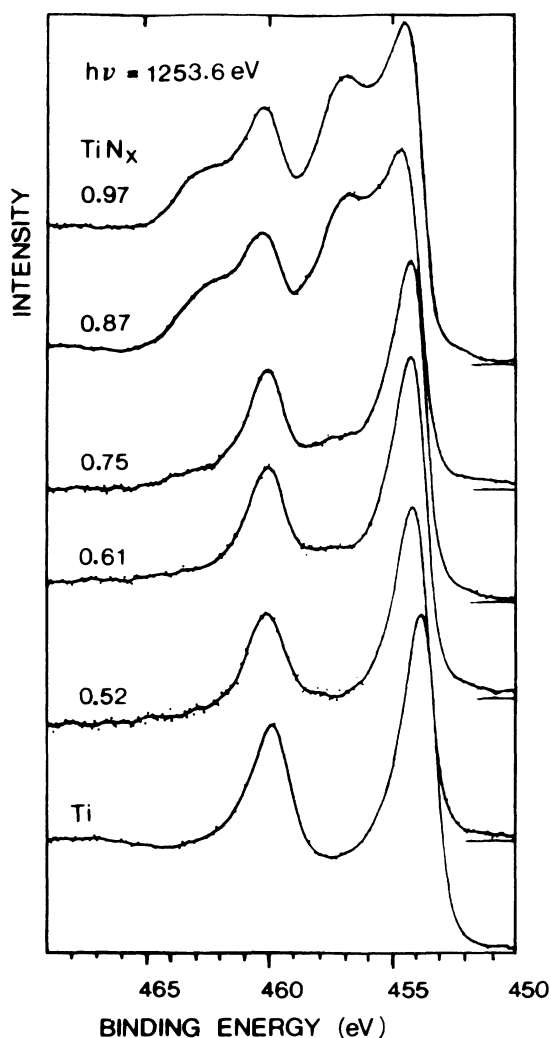


FIG. 6. Ti 2*p* XPS spectra from TiN<sub>x</sub> and from metallic titanium.



tron is transferred from the Fermi level to the localized "screening" state, the total energy of the final state will be lowered thus giving the "well-screened" main XPS peak. If not, the total energy of the final state will be higher, giving the "poorly-screened" satellite XPS peak. The screening will depend on the coupling of the localized screening state to the other occupied levels of the initial state, and as a corollary to the degree of localization of these levels.

By applying these ideas to our results on  $\text{TiN}_x$ , it seems logical that for lower  $x$  the Ti  $2p$  spectrum exhibits essentially the well-screened  $2p_{1/2-3/2}$  doublet. In this case the number of conduction electrons per metal atom is large enough that we can suppose the electrons associated with the vacancy band to be very effective in the screening process. As a matter of fact, band-structure calculations on  $\text{Nb}_{0.75}\text{O}_{0.75}$  have found that the vacancy band has an energy dispersion typical for a nearly-free-electron band.<sup>24</sup> The question now arises as to the reason for the occurrence of Ti  $2p$  satellite structures which appear for the higher  $x$  value. According to our results, the appearance of satellites seems to be strongly dependent on the composition parameter  $x$  for  $\text{TiN}_x$ . The limiting condition for the occurrence of satellite structures can be roughly estimated as  $x \geq 0.8$ . As seen from the evolution of the valence-band spectra, the decrease in the number of vacancies affects primarily the total number of conduction electrons, and more specifically, the number of electrons in the vacancy band. It is clear that decreasing the number of vacancies must lead to a situation when the vacancy states can no longer form a band, and thus must become localized. The critical concentration for this transition depends on the extension of the vacancy states over the lattice. Cluster calculation on NbC (Ref. 25) shows that the states associated with an anion vacancy do not extend beyond the six near-neighbor metal atoms, revealing that this resonant vacancy state is strongly localized in real space within a radius of about one lattice constant. The sudden appearance of strong Ti  $2p$  satellites suggests that the ability of the Ti  $3d$  electrons to screen the core hole created during the XPS process decreases discontinuously with increasing N content. A plausible explanation for the evolution of the satellite structure is as follows: As long as vacancies are in sufficient number to allow overlapping of the wave function and formation of a band, the screening of the core hole will be good. But when the number of vacancies becomes too small, overlapping cannot extend over the entire crystal and vacancy states become localized in the vacancy sites. The probability of core-hole screening drops dramatically, with a corresponding increase in the intensity of

the unscreened final-state satellite. Although the decrease in the total number of electrons in the conduction band as  $x$  increases would also act to reduce the screening probability, the sudden appearance of the satellite structures seems to demand a discontinuous change in behavior of conduction electrons. It is noteworthy that the vacancy concentration corresponding to the appearance of the satellite lines is of the order that would be obtained by applying the simple percolation-model approach<sup>55</sup> to the localized-delocalized transition of the vacancy states.

There are two other important causes of appearance of satellites in XPS core-level spectra that could be pointed out, namely, plasmon excitation and exchange coupling. The sudden appearance of the satellites seems rather difficult to reconcile with a plasmon-excitation process. Moreover, the excitation of a plasmon giving a satellite line at  $\hbar\omega$  from the main line should be accompanied by the excitation of a second plasmon giving a satellite at  $2\hbar\omega$  from the main line. The intensity of the satellite structures suggests the second plasmon excitation would be detectable, but no evidence of this is found in the spectra. Localization of valence electrons may induce the splitting of core signals by exchange coupling with the core hole. This effect has been well characterized in compounds with almost fully localized, unpaired, valence electrons.<sup>53</sup> However, exchange splittings will only appear in a simple form in signals from  $s$  levels. In ionization of core subshells having angular momentum, the exchange coupling competes with the spin-orbit interaction to yield several states, resulting in core-level shapes more complex than those found from the present Ti  $2p$  signals.

#### IV. CONCLUSION

Titanium nitrides  $\text{TiN}_x$  have been investigated by XPS over the entire rocksalt composition range ( $0.5 \leq x \leq 1$ ). The valence-band spectrum of stoichiometric TiN is consistent with the DOS obtained by APW calculations, but the intensity of the hybridized N  $2p$ -Ti  $3d$  band is stronger than expected from atomic cross-section data. The valence-region spectra of the substoichiometric compounds show an increase in the number of electrons above the N  $2p$ -like valence band with decreasing  $x$ . However, this variation is due largely to increasing occupation of a defect state some 2 eV below the Fermi energy, rather than the filling of a "rigid" conduction band as the nitrogen vacancy concentration increases. Comparison of the spectra with various theoretical approaches to anion-deficient materials shows that cluster and APW calculations provide a

good description of the defect states in such compounds.

The variation of N 1s and Ti 2p binding energies with stoichiometry demonstrates a decrease in the ionicity in  $TiN_x$  as nitrogen atoms are removed. The Ti 2p core lines exhibit, in addition, satellite structure for nearly stoichiometric compounds. They are tentatively correlated with a decrease in the screening ability of the conduction electron when the composition approaches the stoichiometric value.

#### ACKNOWLEDGMENTS

We are very indebted to A. Aubert and J. Chevallier (LEMM-Centre d'Etudes Nucléaires de Grenoble) for providing some of the samples, and to M. Fallavier (IPN-Lyon) for the nuclear reaction analysis of the samples. We also acknowledge Professor Tran Minh Duc for work facilities at the Centre Commun ESCA de l'Université Lyon I. L.P. is very pleased to thank R. E. Egdell for numerous fruitful discussions.

- 
- <sup>1</sup>L. E. Toth, *Transition Metal Carbides and Nitrides* (Academic, New York, 1971), Vol. 7.
- <sup>2</sup>W. S. Williams, in *Progress in Solid State Chemistry*, edited by M. Reiss and J. D. McCalden (Pergamon, New York, 1971), Vol. 6.
- <sup>3</sup>V. Ern and A. C. Switendick, *Phys. Rev.* **137**, 1927 (1965).
- <sup>4</sup>J. B. Conklin, Jr., and D. J. Silversmith, *Int. J. Quantum Chem.* **25**, 243 (1968).
- <sup>5</sup>A. Neckel, P. Rastl, R. Eibler, P. Weinberger, and K. Schwartz, *J. Phys. C* **9**, 579 (1976); Report No. SUP 70017 (unpublished).
- <sup>6</sup>A. Neckel, K. Schwartz, P. Weinberger, R. Eibler, and P. Rastl, *Ber. Bunsenges, Phys. Chem.* **79**, 1053 (1975).
- <sup>7</sup>For a review of band-structure calculations for transition-metal carbides, see J. L. Calais, *Adv. Phys.* **26**, 847 (1977).
- <sup>8</sup>For the carbides see, for example, J. H. Weaver, A. M. Bradshaw, J. F. Van der Veen, F. J. Himpsel, D. E. Eastman, and C. Politis, *Phys. Rev. B* **22**, 4921 (1980), and references therein; also see references in Refs. 13 and 18.
- <sup>9</sup>J. Höchst, R. D. Bringans, P. Steiner, and Th. Wolf, *Phys. Rev. B* **25**, 7183 (1982).
- <sup>10</sup>L. I. Johansson, P. M. Stefan, M. L. Shek, and A. N. Christensen, *Phys. Rev. B* **22**, 1032 (1980).
- <sup>11</sup>W. K. Schubert, R. N. Shelton, and E. L. Wolf, *Phys. Rev. B* **23**, 5097 (1981); **24**, 6278 (1981).
- <sup>12</sup>L. I. Johansson, P. M. Stefan, M. L. Shek, and A. N. Christensen, *Solid State Commun.* **36**, 965 (1980).
- <sup>13</sup>L. I. Johansson, A. Callenäs, P. M. Stefan, A. N. Christensen, and K. Schwartz, *Phys. Rev. B* **24**, 1883 (1981).
- <sup>14</sup>J. E. Holliday, *J. Phys. Chem. Solids* **32**, 1825 (1975).
- <sup>15</sup>V. V. Nemoskalenko, V. P. Krivitskii, A. P. Nesenjuk, L. I. Nicolajev, and A. P. Shpak, *J. Phys. Chem. Solids* **36**, 277 (1975).
- <sup>16</sup>D. W. Fischer, *J. Appl. Phys.* **41**, 3922 (1970).
- <sup>17</sup>L. Ramqvist, B. Ekstig, E. Källme, E. Noreland, and R. Manne, *J. Phys. Chem. Solids* **30**, 1849 (1969).
- <sup>18</sup>A. Balzarotti, M. de Crescenzi, and L. Incoccia, *Phys. Rev. B* **25**, 6349 (1982).
- <sup>19</sup>A. Schlegel, P. Wachter, J. J. Nickl, and H. Lingg, *J. Phys. C* **10**, 4889 (1977).
- <sup>20</sup>R. Rivory, J. M. Behaghel, S. Berthier, and J. Lafait, *Thin Solid Films* **78**, 161 (1981).
- <sup>21</sup>P. Steiner, H. Höchst, J. Schneider, S. Hüfner, and C. Politis, *Z. Phys. B* **33**, 241 (1979).
- <sup>22</sup>H. Ihara and K. Watanabe, *Solid State Commun.* **38**, 1211 (1981).
- <sup>23</sup>L. M. Huisman, A. E. Carlsson, C. D. Gelatt, Jr., and H. Ehrenreich, *Phys. Rev. B* **22**, 991 (1980).
- <sup>24</sup>E. Wimmer, K. Schwartz, R. Podloucky, P. Herzog, and A. Neckel, *J. Phys. Chem. Solids* **43**, 439 (1982).
- <sup>25</sup>G. Ries and H. Winter, *J. Phys. F* **10**, 1 (1980).
- <sup>26</sup>J. Klima, *J. Phys. C* **12**, 3691 (1979).
- <sup>27</sup>B. M. Klein, D. A. Papaconstantopoulos, and L. L. Boyer, *Phys. Rev. B* **22**, 1946 (1980).
- <sup>28</sup>H. Höchst, P. Steiner, S. Hüfner, and C. Politis, *Z. Phys. B* **37**, 27 (1980).
- <sup>29</sup>A. L. Hagström, L. I. Johansson, S. B. M. Hagström, and A. N. Christensen, *J. Electron. Spectrosc. Relat. Phenom.* **11**, 75 (1977).
- <sup>30</sup>L. I. Johansson, A. L. Hagström, B. E. Jacobson, and S. B. M. Hagström, *J. Electron. Spectrosc. Relat. Phenom.* **10**, 259 (1977).
- <sup>31</sup>The samples were prepared by J. Chevallier and optical data are found in G. Chassaing, J. C. Francois, P. Gravier, M. Sigrist, L. Roux, and J. Chevallier, in *Proceedings of the 8th International Vacuum Congress, Cannes, France, 1980*, edited by F. Abèles and M. Croset (SFV, Paris, 1980); L. Roux, J. Hanus, J. C. Francois, and M. Sigrist, *Sol. Energy Mater.* **7**, 299 (1982).
- <sup>32</sup>L. Porte, M. Demosthenous, and T. M. Duc, *J. Less-Common Met.* **56**, 183 (1977).
- <sup>33</sup>U. Gelius, in *Electron Spectroscopy*, edited by D. A. Shirley (North-Holland, Amsterdam, 1972), p. 311.
- <sup>34</sup>J. H. Scofield, *J. Electron. Spectrosc. Relat. Phenom.* **8**, 129 (1976).
- <sup>35</sup>S. M. Goldberg, C. S. Fadley, and S. Kono, *J. Electron.*

- Spectrosc. Relat. Phenom. 21, 285 (1981).
- <sup>36</sup>J. Klima, Czech. J. Phys. B 30, 905 (1980).
- <sup>37</sup>K. Schwartz and N. Rösch, J. Phys. C 9, L433 (1976).
- <sup>38</sup>M. Bittner and H. Goretzki, Monash. Chemie 93, 1001 (1962).
- <sup>39</sup>K. Schwartz, J. Phys. C 10, 195 (1977).
- <sup>40</sup>L. Ramqvist, K. Hamrin, G. Johansson, A. Fahlman, and C. Nordling, J. Phys. Chem. Solids 30, 1835 (1969).
- <sup>41</sup>D. Simon, C. Perrin, J. Bardolle, C. R. Acad. Sci. Paris C 283, 299 (1976).
- <sup>42</sup>L. Ramqvist, K. Hamrin, G. Johansson, U. Gelius, and C. Nordling, J. Phys. Chem. Solids 31, 2669 (1970).
- <sup>43</sup>S. P. Denker, J. Less-Common Met. 14, 1 (1968).
- <sup>44</sup>L. Porte, M. Demosthenous, G. Hollinger, Y. Jugnet, P. Pertosa, and T. M. Duc in *Proceedings of the 7th Vacuum Congress and 3rd International Conference on Solid Surfaces, Vienna, 1977*, edited by R. Dobrozemsky (R. Dobrozemsky, Vienna, 1977), p. 923.
- <sup>45</sup>L. Porte (unpublished).
- <sup>46</sup>J. N. Chazalviel, M. Campagna, G. K. Wertheim, and H. R. Shanks, Phys. Rev. B 16, 697 (1977).
- <sup>47</sup>B. A. De Angelis and M. Shiavello, Chem. Phys. Lett. 38, 155 (1976); 58, 249 (1978).
- <sup>48</sup>N. Beatham, P. A. Cox, R. G. Egdell, and A. F. Orchard, Chem. Phys. Lett. 69, 479 (1980).
- <sup>49</sup>J. C. Fuggle, M. Campagna, Z. Zolnierrek, R. Lässer, and A. Platau, Phys. Rev. Lett. 45, 1597 (1980).
- <sup>50</sup>J. C. Fuggle and Z. Zolnierrek, Solid State Commun. 38, 799 (1981).
- <sup>51</sup>S. Hüfner and G. K. Wertheim, Phys. Lett. 51A, 299 (1975).
- <sup>52</sup>G. K. Wertheim, Chem. Phys. Lett. 65, 377 (1979).
- <sup>53</sup>D. A. Shirley, in *Photoemission in Solids*, edited by M. Cardona and L. Ley (Springer, Berlin, 1979), Chap. 4, p. 165.
- <sup>54</sup>J. Friedel, Comments Solid State Phys. 2, 21 (1969).
- <sup>55</sup>V. K. S. Shante and S. Kirkpatrick, Adv. Phys. 20, 325 (1970).